Analysis of imaging data on the population structure, vertical distribution, and growth of two dominant planktonic copepod species in the western subarctic Pacific (#118110)

First submission

Guidance from your Editor

Please submit by **24 May 2025** for the benefit of the authors (and your token reward) .

Structure and Criteria
Please read the 'Structure and Criteria' page for guidance.

Raw data check
Review the raw data.

Image check
Check that figures and images have not been inappropriately manipulated.

If this article is published your review will be made public. You can choose whether to sign your review. If uploading a PDF please remove any identifiable information (if you want to remain anonymous).

Files
Download and review all files from the materials page.

7 Figure file(s)
1 Table file(s)
1 Raw data file(s)

Structure and Criteria

Structure your review

The review form is divided into 5 sections. Please consider these when composing your review:

1. **BASIC REPORTING**
2. **EXPERIMENTAL DESIGN**
3. **VALIDITY OF THE FINDINGS**
4. General comments
5. Confidential notes to the editor

You can also annotate this PDF and upload it as part of your review

When ready submit online.

Editorial Criteria

Use these criteria points to structure your review. The full detailed editorial criteria is on your guidance page.

BASIC REPORTING

- Clear, unambiguous, professional English language used throughout.
- Intro & background to show context. Literature well referenced & relevant.
- Structure conforms to PeerJ standards, discipline norm, or improved for clarity.
- Figures are relevant, high quality, well labelled & described.
- Raw data supplied (see PeerJ policy).

EXPERIMENTAL DESIGN

- Original primary research within Scope of the journal.
- Research question well defined, relevant & meaningful. It is stated how the research fills an identified knowledge gap.
- Rigorous investigation performed to a high technical & ethical standard.
- Methods described with sufficient detail & information to replicate.

VALIDITY OF THE FINDINGS

- **Impact and novelty is not assessed.** Meaningful replication encouraged where rationale & benefit to literature is clearly stated.
- All underlying data have been provided; they are robust, statistically sound, & controlled.
- Conclusions are well stated, linked to original research question & limited to supporting results.

Standout reviewing tips

The best reviewers use these techniques

Tip	*Example*
Support criticisms with evidence from the text or from other sources	*Smith et al (J of Methodology, 2005, V3, pp 123) have shown that the analysis you use in Lines 241-250 is not the most appropriate for this situation. Please explain why you used this method.*
Give specific suggestions on how to improve the manuscript	*Your introduction needs more detail. I suggest that you improve the description at lines 57- 86 to provide more justification for your study (specifically, you should expand upon the knowledge gap being filled).*
Comment on language and grammar issues	*The English language should be improved to ensure that an international audience can clearly understand your text. Some examples where the language could be improved include lines 23, 77, 121, 128 – the current phrasing makes comprehension difficult. I suggest you have a colleague who is proficient in English and familiar with the subject matter review your manuscript, or contact a professional editing service.*
Organize by importance of the issues, and number your points	*1. Your most important issue* *2. The next most important item* *3. …* *4. The least important points*
Please provide constructive criticism, and avoid personal opinions	*I thank you for providing the raw data, however your supplemental files need more descriptive metadata identifiers to be useful to future readers. Although your results are compelling, the data analysis should be improved in the following ways: AA, BB, CC*
Comment on strengths (as well as weaknesses) of the manuscript	*I commend the authors for their extensive data set, compiled over many years of detailed fieldwork. In addition, the manuscript is clearly written in professional, unambiguous language. If there is a weakness, it is in the statistical analysis (as I have noted above) which should be improved upon before Acceptance.*

Analysis of imaging data on the population structure, vertical distribution, and growth of two dominant planktonic copepod species in the western subarctic Pacific

Tian Gao [1], **Atsushi Yamaguchi** [Corresp. 1, 2]

[1] Graduate School of Fisheries Sciences, Hokkaido University, Hakodate, Hokkaido, Japan

[2] Arctic Research Center, Hokkaido University, Sapporo, Hokkaido, Japan

Corresponding Author: Atsushi Yamaguchi
Email address: a-yama@fish.hokudai.ac.jp

Traditionally, zooplankton analyses have relied on stereomicroscopes, but recent advancements in imaging analysis have offered significant advantages, including the simultaneous collection of abundance, size, and biovolume data. In this study, formalin-preserved samples were collected from depths of 0 to 1000 m across four seasons at a station in the western subarctic Pacific, using the imaging device ZooScan. Two dominant copepod genera, *Metridia* and *Eucalanus*, were examined for seasonal changes in abundance, biovolume, and diurnal vertical distribution. ZooScan measurements for each developmental stage were taken to calculate intermolt growth based on the equivalent spherical diameter (ESD) and biovolume. Four *Metridia* species were identified: *M. pacifica*, *M. okhotensis, M. asymmetrica*, and *M. curticauda. M. pacifica*, the dominant species, had an ESD of 2 mm or less, while the other three species exceeded 2 mm. *M. pacifica* exhibited diurnal migration to surface layers (0–50 m) at night, while the larger species were primarily located in the deeper layer (750–1000 m) both day and night. Only one species, *E. bungii*, was identified in the genus *Eucalanus*, with size cohorts corresponding to each developmental stage. Its vertical distribution was consistent day and night across seasons, but seasonal changes were evident. In October and February, *E. bungii* was found at depths of 200–500 m. In April, later developmental stages migrated to shallower depths of 50–200 m, while in July, younger stages (C1–C4) were found at 0–50 m, indicating recent reproduction during the spring phytoplankton bloom. The generation time of *E. bungii* varies from 1 to 3 years. Although it was clear that new individuals emerged in July, understanding the dynamics of later stages and generation time was difficult due to overlapping size distributions, particularly in C5 and C6. Inter-molt growth for *M. pacifica* ranged from 6.7% to 40.4% based on ESD and from 21.1% to 177.8% based on biovolume. For *E. bungii*, these ranges were 6.2% to 48.2% and 18.5% to 223.5%, respectively, with biovolume growth being significantly higher. Both species showed differences in inter-molt

growth between males and females, with females being larger. Notably, *M. pacifica* has functional mandible teeth in C6M, while *E. bungii* C6M's teeth are degenerate. *M. pacifica* C6F exhibits significant vertical migration to the surface at night, unlike C6M, which remains deeper. This difference in behavior likely impacts feeding conditions, contributing to the lower inter-molt growth rates for male stages.

Analysis of imaging data on the population structure, vertical distribution, and growth of two dominant planktonic copepod species in the western subarctic Pacific

Tian Gao[1] and Atsushi Yamaguchi[1,2,*]

[1]Graduate School of Fisheries Sciences, Hokkaido University, 3–1–1 Minato-cho, Hakodate, Hokkaido, 041–8611, Japan
[2]Arctic Research Center, Hokkaido University, Kita-21 Nishi-11 Kita-ku, Sapporo, Hokkaido, 001-0021, Japan
*Corresponding author: a-yama@fish.hokudai.ac.jp (Atsushi Yamaguchi)

Abstract:
Traditionally, zooplankton analyses have relied on stereomicroscopes, but recent advancements in imaging analysis have offered significant advantages, including the simultaneous collection of abundance, size, and biovolume data. In this study, formalin-preserved samples were collected from depths of 0 to 1000 m across four seasons at a station in the western subarctic Pacific, using the imaging device ZooScan. Two dominant copepod genera, *Metridia* and *Eucalanus*, were examined for seasonal changes in abundance, biovolume, and diurnal vertical distribution. ZooScan measurements for each developmental stage were taken to calculate intermolt growth based on the equivalent spherical diameter (ESD) and biovolume. Four *Metridia* species were identified: *M. pacifica, M. okhotensis, M. asymmetrica,* and *M. curticauda*. *M. pacifica*, the dominant species, had an ESD of 2 mm or less, while the other three species exceeded 2 mm. *M. pacifica* exhibited diurnal migration to surface layers (0–50 m) at night, while the larger species were primarily located in the deeper layer (750–1000 m) both day and night. Only one species, *E. bungii*, was identified in the genus *Eucalanus,* with size cohorts corresponding to each developmental stage. Its vertical distribution was consistent day and night across seasons, but seasonal changes were evident. In October and February, *E. bungii* was found at depths of 200–500 m. In April, later developmental stages migrated to shallower depths of 50–200 m, while in July, younger stages (C1–C4) were found at 0–50 m, indicating recent reproduction during the spring phytoplankton bloom. The generation time of *E. bungii* varies from 1 to 3 years. Although it was clear that new individuals emerged in July, understanding the dynamics of later stages and generation time was difficult due to overlapping size distributions, particularly in C5 and C6. Inter-molt growth for *M. pacifica* ranged from 6.7% to 40.4% based on ESD and from 21.1% to 177.8% based on biovolume. For *E. bungii*, these ranges were 6.2% to 48.2% and 18.5% to 223.5%, respectively, with biovolume growth being significantly higher. Both species showed differences in inter-molt growth between males and females, with females being larger. Notably, *M. pacifica* has functional mandible teeth in C6M, while *E. bungii* C6M's teeth are degenerate. *M. pacifica* C6F exhibits significant vertical migration to the surface at night, unlike C6M, which remains deeper. This difference in behavior likely impacts feeding conditions, contributing to the lower inter-molt growth rates for male stages.

Subjects: Ecology, Marine Biology, Zoology

Keywords: DVM, *Eucalanus*, Life cycle, *Metridia,* SVM, ZooScan

Introduction

In the western subarctic Pacific, St. K2 has been established as a long-term time-series observation station by Japan Agency for Marine-Earth Science and Technology (JAMSTEC). The quantification and flux of various biogeochemical parameters from this station have been reported (Honda et al., 2017). Research on zooplankton at St. K2 has provided several key findings, including estimates of vertical carbon flux to the deep layers achieved through the ontogenetic vertical migration of large-sized copepods as they enter diapause (Kobari et al., 2008). Other studies have compared zooplankton communities at St. K2 with those at subtropical stations (Steinberg et al., 2008a) and estimated the consumption of sinking particles by

mesozooplankton and heterotrophic bacteria in the deep layers (Steinberg et al., 2008b). Additionally, the community structure of zooplankton at St. K2 has been analyzed in comparison to subtropical stations (Kitamura et al., 2016), and seasonal changes in zooplankton collected from time-series sediment traps at a depth of 200 m have been documented (Yokoi et al., 2018). While these findings are significant, most have focused on elucidating community structure and material circulation, leaving a gap in our understanding of the dynamics and population structure of dominant species within each zooplankton taxonomic group. To address this gap, examples of species-level analyses have been conducted using vertically stratified samples collected both during the day and night across four seasons. Amei et al. (2021) analyzed pelagic polychaetes, while Taniguchi et al. (2023) focused on pelagic amphipods. Additionally, two other studies have documented seasonal changes in population structure, including body size and gonadal development of dominant species, such as the chaetognath *Eukrohnia hamata* (Nakamura, Zhang & Yamaguchi, 2023) and the hydromedusa *Aglantha digitale* (Aizawa, Gao & Yamaguchi, 2023).

Recent studies on zooplankton at St. K2 have shifted from traditional stereomicroscopes to advanced imaging techniques. A standout innovation is ZooScan, developed in the 2000s, which measures individual zooplankton size and identifies their species from images, proving effective in various marine ecosystems (Gorsky et al., 2010; Irisson et al., 2022). At St. K2, ZooScan is used particularly for analyzing pelagic amphipods (Taniguchi et al., 2023). In their study, Taniguchi et al. (2023) utilized ZooScan on amphipod samples sorted with a stereomicroscope, enabling detailed assessments of population structure in terms of both abundance and biovolume. For the dominant species, *Themisto pacifica*, they analyzed growth and dynamics based on the equivalent spherical diameter (ESD). The advantages of ZooScan for in-depth analysis of specific planktonic taxa are increasingly clear and could enhance our understanding of marine biodiversity.

Copepods are the most dominant group in terms of both abundance and biomass within the zooplankton community of the western subarctic Pacific (Ikeda, Shiga & Yamaguchi, 2008). The large-sized copepod genus *Neocalanus* is particularly notable for its biomass, comprising three sympatric species: *N. cristatus, N. flemingeri,* and *N. plumchrus* (Kobari & Ikeda, 2000). Identifying these three species requires the use of a stereomicroscope, making it challenging to discern them from imaging data obtained through other instruments. In addition to *Neocalanus, Metridia pacifica* and *Eucalanus bungii* are two copepod species that also have significant biomass and large body sizes (Ikeda, Shiga & Yamaguchi, 2008). The life cycles of these two species have been documented in the Oyashio region of the western North Pacific subarctic (Padmavati, Ikeda & Yamaguchi, 2004; Shoden, Ikeda & Yamaguchi, 2005) and in the Gulf of Alaska in the eastern North Pacific subarctic (Miller et al., 1984; Batchelder, 1985). However, these studies relied on microscopic data gathered with a stereomicroscope, and no imaging analyses have been conducted to explore the dynamics of these two species.

Imaging analysis of zooplankton offers several advantages, allowing researchers to simultaneously gather not only abundance data but also information on size (equivalent spherical diameter, ESD) and biovolume. When analyzing the entire zooplankton community, researchers can calculate a Normalized Biovolume Size Spectrum (NBSS), with zooplankton size represented on the horizontal axis and biovolume on the vertical axis. This analysis enables the evaluation of energy transport efficiency to higher organisms, such as fish (Naito et al., 2019; Teraoka et al., 2022). For copepods, imaging analysis can be performed on samples sorted by copepodite stage, allowing for the measurement of both ESD and biovolume for each stage. Traditionally, the intermolt growth of copepodite stages has been assessed using body length and dry weight (Mauchline, 1998). However, with the use of imaging equipment like ZooScan, it is now possible to evaluate intermolt growth through ESD and biovolume. Understanding these characteristics is increasingly important as imaging analysis becomes more widespread.

In this study, we conducted ZooScan measurements on formalin-preserved zooplankton samples collected from vertical stratified sites at depths ranging from 0 to 1000 meters at Station K2 during four consecutive seasons. We identified two large copepod species: *Metridia* spp. and *E. bungii*, based on the images obtained. Our analysis focused on seasonal changes in the abundance and vertical distribution of the biovolume of these species, as well as the size spectra measured in equivalent spherical diameter (ESD) units. Additionally, we sorted *M. pacifica* and *E. bungii* from the formalin-preserved samples according to

each copepodite stage. ZooScan measurements were performed on each stage to assess intermolt growth, analyzing the ESD and biovolume for each copepodite stage to evaluate growth characteristics related to body size and biovolume.

Materials and Methods

Field sampling

On October 29, 2010, February 26, April 22, and July 3–4, 2011, we conducted day and night vertically stratified oblique tows using a multi-stage open-close net system called IONESS (Intelligent Operative Net Sampling System, SEA Co. Ltd.) with a mesh size of 335 µm and an opening area of 1.5 m². The net was divided into eight layers corresponding to depths of 0–50 m, 50–100 m, 100–150 m, 150–200 m, 200–300 m, 300–500 m, 500–750 m, and 750–1000 m, at Station K2 (47°N, 160°E; depth 5230 m) in the western subarctic Pacific (see Table 1). The collected samples were immediately preserved on board the ship using 5% borax-buffered formalin in seawater. During each sampling period, environmental data, including water temperature, salinity, dissolved oxygen concentration, and fluorescence, were measured with a CTD (SBE 911 plus; Sea-Bird Electronics Inc.).

ZooScan measurements

In the land laboratory, the zooplankton samples were divided into subsamples ranging from 1/2 to 1/128, depending on the abundance of the zooplankton. Measurements were conducted using the ZooScan imaging device (ZooScan MIII, Hydroptic Inc.), following the methodologies outlined by Gorsky et al. (2010). Initially, the ZooScan scanning cell was filled with distilled water, and a background scan was performed. Next, the zooplankton sample was poured into the scanning cell, and the sample was scanned. During the scanning process, care was taken to adjust the sample's position using a dissection needle or other tools. This was done to prevent the sample from floating on the water surface or to avoid overlap between multiple individual organisms. The scanned images were then segmented into individual images using ZooProcess in ImageJ software. Finally, these images were uploaded to EcoTaxa (http://ecotaxa.obs-vlfr.fr/) via FileZilla to acquire species identification and equivalent spherical diameter (ESD, measured in mm) data for each individual.

Data analysis

Metridia spp. and *E. bungii* dominate the copepod community in terms of both abundance and biomass, and their distinct morphological features make them easy to identify from other species. The *Metridia* genus includes *M. pacifica, M. okhotensis, M. asymmetrica*, and *M. curticauda* (Fig. 2). For each sample, we calculated the abundance (individuals per cubic meter, ind. m^{-3}) and biovolume (cubic millimeters per cubic meter, $mm^3\ m^{-3}$) of both species, as well as the equivalent spherical diameter (ESD), based on the aliquot rate and filtered volume. These abundance and biovolume values were then multiplied by the net towing depth (in meters) to determine the abundance (ind. m^{-2}) and biovolume ($mm^3\ m^{-2}$) per square meter, providing estimates for each depth layer in the water column. To assess the standing stock (abundance throughout the water column), we integrated the abundance (ind. m^{-2}) across all layers of the 0-1000 m water column. The percentage of abundance at each layer was calculated as a proportion of the total standing stock, allowing us to evaluate the vertical distribution of the population. We generated histograms in 0.1 mm ESD intervals to assess the population structure based on the standing stock values within the 0-1000 m water column. Additionally, the vertical distribution was analyzed by examining the percentage of each depth layer in relation to the standing stock values across the 0-1000 m water column, again in 0.1 mm ESD intervals.

For *M. pacifica* and *E. bungii* found in the IONESS samples, individuals were sorted by copepodite stage from their most abundant samples. ZooScan measurements were then taken for each copepodite stage. The mean and standard deviation of the equivalent spherical diameter (ESD) were calculated for each stage. In contrast, for *M. okhotensis, M. asymmetrica*, and *M. curticauda*, ZooScan measurements were conducted solely on adult females (C6F), and the mean and standard deviation of ESD were also calculated for these species.

Intermolt growth of body length and volume

The intermolt growth percentage of body length (Equivalent Spherical Diameter, ESD, in mm) and biovolume (in mm^3 per individual) for each copepodite stage of *M. pacifica* and *E. bungii* was calculated using the following formula (Mauchline, 1998):

Increment (%) = 100 × [(Post-molt size - Pre-molt size) / Pre-molt size]

Additionally, the proportion of growth at each copepodite stage was assessed for both body length (ESD) and volume (biovolume), with the values for adult males and females set at 100% (Yamaguchi et al., 2020).

Results

Hydrological environments

Figure 3 displays the vertical distributions of water temperature, salinity, dissolved oxygen, and fluorescence for each sampling period. Throughout the study, water temperatures ranged from 0.7 to 8.5°C, salinity varied between 32.5 and 34.5, dissolved oxygen concentrations ranged from 0.3 to 7.5 ml L^{-1}, and fluorescence levels ranged from 0.02 to 2.32. A seasonal thermocline was observed at around 50 m in October and June, while in February and April, the temperature remained nearly uniform down to 100 m. Across all sampling periods, the water temperature exhibited a minimum of 1–2°C at depths of 100 m, peaked at approximately 3.5°C around 200 m, and then declined with increasing depth below 200 m. Salinity consistently increased with depth during all seasons, although it was uniform above 100 m in February and April. In June and October, salinity remained low (below 33) at depths above 50 m. Dissolved oxygen (DO) levels decreased with increasing depth; although some concentrations were measured down to 200 m, they dropped to extremely low levels (below 2 ml L^{-1}) at depths greater than 200 m. Fluorescence was predominantly high only above the thermocline during all seasons, with the peak value recorded in June.

Metridia spp.

Figure 4 displays the day and night abundance (ind. m^{-2}) and biovolume (mm3 m-2) of *Metridia* copepods, along with their abundance distribution across eight layers in the 0-1000 m water column, categorized by a 0.1 mm ESD interval. Among the four *Metridia* species studied, *M. pacifica* was smaller, with an ESD below 2 mm. In contrast, the other three *Metridia* species had an ESD greater than 2 mm (Fig. 4). During the day, *M. pacifica* specimens, particularly the larger individuals, were found at greater depths. However, they exhibited a distinct diel vertical migration, rising to the surface layer (0-50 m) at night across all four seasons. In contrast, the remaining three larger *Metridia* species were predominantly located in the deepest layer (750-1000 m) both day and night throughout all seasons. The abundance and biovolume of *Metridia* spp. were observed to be low in February and April but peaked in July and October.

Eucalanus bungii

Fig. 5 illustrates the abundance, biovolume, and vertical distribution composition of *E. bungii* during day and night. Unlike *Metridia* spp., which includes multiple species, *E. bungii* consists of only a single species. Consequently, the size of the cohorts in the ESD corresponds directly to each copepodite stage. There were no diel variations in the vertical distribution of *E. bungii* observed in any season. However, a clear seasonal shift in vertical distribution was noted. In October and February, *E. bungii* was found at depths of 200–500 meters both day and night. In contrast, during April, especially for the later copepodite stages, the distribution became shallower, occurring in the 50–200 m layer both day and night. In July, the younger copepodite stages, specifically those younger than C4, were located in the shallowest layer of 0–50 m both day and night. The highest abundance of *E. bungii* was recorded in October, with the ESD indicating that the developmental stages dominating this period were C5 and C6.

Inter-molt growth

The inter-molt growth of copepodite stages of *M. pacifica* and *E. bungii*, as measured by ESD and biovolume, is illustrated in Fig. 6. For *M. pacifica*, the inter-molt growth in ESD ranged from 6.7% to

40.4%, while for *E. bungii*, it ranged from 6.2% to 48.2%. In contrast, the inter-molt growth based on biovolume was observed to be between 21.1% and 177.8% for *M. pacifica* and between 18.5% and 223.5% for *E. bungii*. Thus, it is evident that inter-molt growth based on biovolume was greatly higher than that based on ESD. A notable observation for both species is that the inter-molt growth in the C5M/C6M stages was considerably lower than in the C5F/C6F stages, regardless of whether measured by ESD or biovolume (Fig. 6).

Figure 7 illustrates the percentage of each copepodite stage, with the equivalent ESD and biovolume of adult females and males (C6F/M) of *M. pacifica* and *E. bungii* set as 100%. Clear differences were observed based on the units of measurement (ESD vs. biovolume) and between sexes. Specifically, regarding ESD, the percentage of C1 and earlier stages was the largest for both females and males across the two species, indicating the importance of body length during early stages. Conversely, when considering biovolume, females showed the highest percentage in the C5/C6 stages, while males exhibited the greatest percentage in the C4/C5 stages. This highlights a significant difference between the sexes: in females, the largest growth occurs at C5/C6 during the transition to adulthood, while in males, it occurs at C4/C5. These differences in measurements (ESD versus biovolume) and between sexes were consistent across both species.

Discussion

Metridia spp.

Studies conducted at depths of 1000 m or more in the subarctic Pacific and its marginal seas have reported the presence of seven (Homma & Yamaguchi, 2010) or nine (Yamaguchi et al., 2002) species within the genus *Metridia*. The most common species is *M. pacifica*, which ranks as the second most abundant species among all calanoid copepods, following *Microcalanus pygmaeus* (Yamaguchi et al., 2002; Homma & Yamaguchi, 2010). The life cycle of *M. pacifica* has been observed in various locations, including the Gulf of Alaska in the eastern subarctic Pacific (Batchelder, 1985), Toyama Bay in the Japan Sea (Hirakawa & Imamura, 1993), and the Oyashio region in the western subarctic Pacific (Padmavati, Ikeda & Yamaguchi, 2004). The number of generations per year varies by location: in Toyama Bay, only one generation is produced annually (Hirakawa & Imamura, 1993), while two generations occur in the Oyashio region (Padmavati, Ikeda & Yamaguchi, 2004), and three generations take place in the Gulf of Alaska. In this study, collections occurred only four times over one year (Table 1), which made it challenging to analyze the precise life cycle. However, during all four observational periods (October, February, April, and July), *M. pacifica* populations exhibited clear diel vertical migration (DVM), ascending to the surface layer at depths of 0–50 meters during the night (Fig. 4). Additionally, *M. pacifica* populations are known to undergo a diapause period, during which they remain in deeper waters and do not migrate to the surface layer both day and night in Toyama Bay and the Oyashio region (Hirakawa & Imamura, 1993; Padmavati, Ikeda & Yamaguchi, 2004). Based on these observations, it is interpreted that *M. pacifica* in the western subarctic Pacific, where this study was conducted, does not experience a diapause period. Its life cycle appears to resemble that of the population in the Gulf of Alaska, which has repeat generations throughout the year (Batchelder, 1985).

Various studies have indicated that the daytime vertical distribution of *M. pacifica* has shifted to a deeper layer as the organisms develop (Hattori, 1989; Sato et al., 2011). In terms of the ontogenetic changes that occur, wherein the daytime distribution depth increases as the copepodite stages progress, Takahashi et al. (2009) observed seasonal variations in the daytime vertical distribution of *M. pacifica* and *M. okhotensis* in the Oyashio region. They found that the daytime distribution depth of late copepodite stages (C4–C6F), which occur at depths ranging from 100 to 400 m, is correlated with the depths of the euphotic zone, which lies between 10 and 60 m at the surface. Takahashi et al. (2009) clarified that when the euphotic zone is shallow—characterized by abundant surface phytoplankton that blocks light from penetrating deeper—the distribution of late copepodite stages is also shallow. Conversely, when the euphotic zone is deep, indicating a scarcity of surface phytoplankton and greater light penetration into the deep sea, the distribution of late copepodite stages tends to be deeper. They posited that the deeper daytime distribution of larger late copepodite stages is to avoid predation by visual predators, such as pelagic fish.

This study also observed that the increase in daytime distribution depth coincides with the later copepodite stages of *M. pacifica* (Fig. 4).

Eucalanus bungii

In studies conducted on pelagic copepods at depths of 1000 m or more in the subarctic Pacific and its marginal seas, *Eucalanus bungii* is the only species from the genus *Eucalanus* identified in this region (Yamaguchi et al., 2002; Homma & Yamaguchi, 2010). The size cohorts observed in ESD of *E. bungii* correspond clearly to each copepodite stage, specifically stages C1–C6F/M (Fig. 5). However, from the C4 stage onward, *E. bungii* can be morphologically distinguished between females and males. Males possess a small fifth leg, while females do not (Fig. 2b). Although the body size (ESD) of the C6F stage is notably different from that of C6M, the ESD of females and males overlaps for the C4 and C5 stages (Fig. 5). This overlap makes it challenging to confirm the presence or absence of the small fifth leg in images (Fig. 2b). Additionally, the ESD of small adult C6M overlaps with that of C5F/M (Fig. 5). Considering these factors, it becomes difficult to accurately identify the copepodite stage of *E. bungii* using ESD alone, particularly for the later copepodite stages.

The life cycle of *E. bungii* has been reported in various regions, including the fjords of British Columbia, Canada (Krause & Lewis, 1979), the Gulf of Alaska in the eastern subarctic Pacific (Miller et al., 1984), and the Oyashio region in the western subarctic Pacific (Tsuda, Saito & Kasai, 2004; Shoden, Ikeda & Yamaguchi, 2005). *E. bungii* experiences a deep-sea diapause period during several late copepodite stages, with generation times reported as 1–2 years in the Oyashio region (Tsuda, Saito & Kasai, 2004; Shoden, Ikeda & Yamaguchi, 2005) and 2–3 years in the Gulf of Alaska (Miller et al., 1984). In both regions, the diapause period occurs from October to March of the following year, although there are regional differences in the distribution depths during this period: 250–500 meters in the Gulf of Alaska (Miller et al., 1984) and deeper than 500 meters in the Oyashio region (Shoden, Ikeda & Yamaguchi, 2005).

The vertical distribution of *E. bungii* observed in this study showed a concentration at depths of 200–500 meters both during the day and night in October and February. Individuals were rarely found below 500 meters, with developmental stages C3 and later being dominant (Fig. 5). The vertical distribution of these diapause individuals of *E. bungii* in the western subarctic Pacific is very similar to that of the population in the Gulf of Alaska, as previously mentioned (Miller et al., 1984). This consistency aligns with the characteristics of the life cycle of *M. pacifica* in the Gulf of Alaska. The vertical distribution of *E. bungii* exhibited seasonal changes, particularly during the late copepodite stages. In April, individuals were found at shallower depths of 50–200 meters both day and night (Fig. 5). This behavioral shift indicates that individuals that were dormant in deeper waters begin to awaken and ascend to shallower layers during the spring phytoplankton bloom period. This phenomenon has been documented in both the Gulf of Alaska (Miller et al., 1984) and the Oyashio region (Yamaguchi et al., 2010a, 2010b). A short-term time series of daily observations on zooplankton was conducted at one station in the Oyashio region from March to April (Yamaguchi et al., 2010a). During this study, vertical stratified sampling was conducted five times over 9-day intervals from depths of 0 to 1000 m (Yamaguchi et al., 2010b). It was noted that from March to April, the gonads of *E. bungii* C6F began to develop, egg production commenced, and nauplii started to recruit (Yamaguchi et al., 2010a). Initially, at the beginning of the study, all individuals were located at their diapause depth during both day and night. However, by the second and third sampling periods, they had migrated to the surface, showing no difference in vertical distribution between day and night. This upward migration began first with the late copepodite stage, specifically C6F (Yamaguchi et al., 2010b). In April, although the fluorescence values, which indicate phytoplankton abundance, were low, the population of *E. bungii* had started to migrate upward to shallower layers during the late copepodite stage. This upward movement was not observed during the dormant periods in October or February. This suggests that copepods with a multi-year generation length, such as *E. bungii*, may possess an internal clock that prompts them to awaken from dormancy at depth and triggers upward migration (cf. Mauchline, 1998).

In July of this study, all copepodite stages of *E. bungii* (C1–C6F) were present. The early copepodite stages were found in the surface layer, ranging from 0 to 50 m, both during the day and at night (Fig. 5). Adult males (C6M), nauplii, and the early copepodite stages C1 and C2 of *E. bungii* were observed

only during a limited seasonal window within a year. In contrast, the diapause developmental stages C3–C6F were present year-round, which is consistent across all the marine areas examined in this study (Miller et al., 1984; Tsuda, Saito & Kasai, 2004; Shoden, Ikeda & Yamaguchi, 2005). This study successfully created a histogram of body length (ESD) for exclusively *E. bungii*, allowing for a clear distinction of the population structure among the early developmental stages (C1–C4F/M) without overlap between the stages. However, distinguishing between males and females in the later developmental stages (C5F/M–C6F/M), and even stage C4, proved challenging. While it was evident that growth and the recruitment of new generation recruits through reproduction occurred in July, evaluating the dynamics of the later copepodite stages and understanding the life cycle, especially generation time, remained difficult using only the image analysis data from ZooScan.

Inter-molt growth of copepods

Inter-molt growth in calanoid copepods has been extensively reviewed, highlighting data from 12 to 94 species at each copepodite stage (Mauchline, 1998). The findings indicate that the mean inter-molt growth at each copepodite stage, when expressed in terms of body length (total length or prosome length), ranges from 4.0% to 33.8%. In contrast, the mean inter-molt growth expressed in terms of body weight (either wet weight or dry weight) varies from 10.3% to 94.0%. This suggests that the inter-molt growth relative to body weight is greater than that relative to body length (Mauchline, 1998). In this study, inter-molt growth is analyzed using equivalent spherical diameter (ESD) and biovolume. The results reveal that inter-molt growth measured by ESD ranges from 6.2% to 48.2%, while inter-molt growth measured by biovolume ranges from 18.5% to 223.5%. This indicates that inter-molt growth expressed by volume (which correlates with body weight) is substantially larger than that represented by body length (ESD) (Fig. 6). The difference in inter-molt growth is attributed to the fact that body length is a one-dimensional measure. In contrast, volume and body weight are three-dimensional attributes (Mauchline, 1998).

It is important to note that the intermolt growth rates of the two copepod species examined in this study are higher than those reported by Mauchline (1998). For example, the length-based growth rates in Mauchline (1998) ranged from 4.0% to 33.8%, while this study found rates between 6.2% and 48.2%. Similarly, the volume/weight-based growth rates reported by Mauchline (1998) were between 10.3% and 94.0%, compared to 18.5% to 223.5% in the current study. The differences in growth rates are likely due to the copepod data collected in Mauchline (1998), which primarily involved small, coastal, and epipelagic species with shorter generations. In contrast, the two copepod species studied here are larger, oceanic species with longer generations. Indeed, previous research has reported extremely high maximum intermolt growth rates based on body mass (either dry weight [DW] or ash-free dry weight [AFDW]) for large deep-sea copepods that inhabit cold environments and have long generation lengths. For instance, growth rates of 295% (Yamaguchi & Ikeda, 2000a), 339.6% (Koguchi et al., 2023), 358.8% (Yamaguchi et al., 2020), 418.6% (Yamaguchi & Ikeda, 2002), 498% (Yamaguchi & Ikeda, 2000b), 531% (Ikeda & Hirakawa, 1996), and 683.2% (Yamaguchi et al., 2019) have been documented. These findings suggest that intermolt growth in copepods varies significantly depending on their habitat. Small species with short generation lengths living in warm coastal and surface waters exhibit limited intermolt growth, while larger species with longer generation lengths in oceanic and deep-sea environments show substantial intermolt growth. In this context, the results of this study align with the observation that *E. bungii*, which has a long generation length, demonstrated greater intermolt growth than *M. pacifica*, which has a shorter generation length (Fig. 6).

A common characteristic observed in the inter-molt growth of both species, *M. pacifica* and *E. bungii*, is a noticeable difference between the sexes as they grow to adulthood (C5/C6). Females tend to be larger, while males are significantly smaller (see Figs. 6 and 7). In numerous calanoid copepod species, adult males are typically smaller than adult females. Studies have reported that the mean inter-molt growth based on body length at C5/C6 ranges from 23.0% to 23.1% for females and from 4.0% to 14.5% for males (Mauchline, 1998). Research on the inter-molt growth of various deep-sea copepods commonly indicates that females experience substantial growth to adulthood, while males show minimal growth. In some cases, negative growth has been reported in C5M/C6M inter-molt growth based on dry weight (DW) or ash-free dry weight (AFDW) (Yamaguchi & Ikeda, 2000a; Yamaguchi et al., 2020; Koguchi et al., 2023). Deep-sea

copepods, such as those from the family Aetideidae, that exhibit negative growth are believed to have degenerated mandible teeth in C6M, rendering them unable to feed (Yamaguchi et al., 2005 and references therein). Among the two copepod species studied, *M. pacifica* retains functional mandible teeth in C6M, while *E. bungii* displays degeneration of these teeth in C6M (Hiiragi & Yamaguchi, 2019). Furthermore, *M. pacifica* C6M, with its functional mandible teeth, shows a distinct sexual difference in diurnal vertical distribution. While females (C6F) exhibit a clear diel vertical migration (DVM) and ascend to the surface at night, males (C6M) remain in the deep layer throughout the day without ascending (Batchelder, 1985; Hattori, 1989; Padmavati, Ikeda & Yamaguchi, 2004; Yamaguchi et al., 2004, 2010b; Sato et al., 2011). The deep layer is believed to have limited food availability for *M. pacifica*, which feeds on particulates. This reduced feeding environment for C6M, which remains in the deep layer all day, is likely poorer than that of C6F, which migrates to the surface at night. This difference in feeding opportunities may explain why the inter-molt growth of *M. pacifica* C5M/C6M is less than that of C5F/C6F, despite C6M having functional mandible teeth.

Acknowledgements

We would like to express our heartfelt gratitude to Dr. Minoru Kitamura of the Japan Agency for Marine-Earth Science and Technology (JAMSTEC) for collecting and providing the IONESS net samples used in this study, as well as for his valuable suggestions. We also sincerely thank all the researchers involved in the project, including Dr. Makio Honda of JAMSTEC, who served as the K2S1 research project leader. Our thanks also go to the captain and crew of the JAMSTEC research vessel Mirai for their efforts in conducting the offshore work. We also thank the World Association of Copepodologists for being a hub for PeerJ of this manuscript.

Additional information and declarations

Funding

This work was partially supported by the Arctic Challenge for Sustainability II (ArCS II) Program (Grant Number JPMXD1420318865), Grants-in-Aid for Challenging Research (JP20K20573 [Pioneering] to AY), and Scientific Research (JP22H00374 [A] to AY) from the Japanese Society for the Promotion of Science (JSPS).

Grant Disclosures

The following grant information was disclosed by the authors:
Ministry of Education, Culture, Sports, Science and Technology (MEXT)
Japanese Society for the Promotion of Science (JSPS)

Competing Interests

The authors declare that they have no competing interests.

Author Contributions

Tian Gao conceived and designed the studies, performed the measurements, analyzed the data, prepared figures and/or tables, authored or reviewed drafts of the paper, and approved the final draft.
Atsushi Yamaguchi conceived and designed the studies, analyzed the data, authored or reviewed drafts of the paper, and approved the final draft.

Data Availability

The following information was supplied regarding data availability:
The ZooScan data for the analysis are parameters reported in the figures.

Supplemental Information

Supplemental information for this article can be found online after acceptance.

References

Aizawa M, Gao T, Yamaguchi A. 2023. Seasonal changes in vertical distribution and population structure of the dominant hydrozoan *Aglantha digitale* in the western subarctic Pacific. *Oceans* **4(3)**:242–252 DOI 10.3390/oceans4030017.

Amei K, Dobashi R, Jimi N, Kitamura M, Yamaguchi A. 2021. Vertical changes in abundance, biomass and community structure of pelagic polychaetes down to 1000 m depths at Station K2 in the western subarctic Pacific Ocean covering the four seasons and day–night. *Journal of Plankton Research* **43(3)**:442–457 DOI 10.1093/plankt/fbab031.

Arima D, Yamaguchi A, Nobetsu T, Imai I. 2016. Seasonal abundance, population structure, sex ratio and gonad maturation of *Metridia okhotensis* Brodsky, 1950 in the Okhotsk Sea: Analysis of samples collected by pumping up from deep water. *Crustaceana* **89(2)**:151–161 DOI 10.1163/15685403-00003516.

Batchelder HP. 1985. Seasonal abundance, vertical distribution, and life history of *Metridia pacifica* (Copepoda: Calanoida) in the oceanic subarctic Pacific. *Deep Sea Research Part A. Oceanographic Research Papers* **32(8)**:949–964 DOI 10.1016/0198-0149(85)90038-X.

Gorsky G, Ohman MD, Picheral M, Gasparini S, Stemmann L, Romagnan J-B, Cawood A, Pesant S, García-Comas C, Prejger F. 2010. Digital zooplankton image analysis using the ZooScan integrated system. *Journal of Plankton Research* **32(3)**:285–303 DOI 10.1093/plankt/fbp124.

Hattori H. 1989. Bimodal vertical distribution and diel migration of the copepods *Metridia pacifica*, *M. okhotensis*, and *Pleuromamma scutullata* in the western North Pacific Ocean. *Marine Biology* **103(1)**:39–50 DOI 10.1007/BF00391063.

Hiragi M, Yamaguchi A. 2019. Vertical distribution and population structure of large dominant planktonic copepods down to greater depths in the Okhotsk Sea during early summer. *Bulletin of Fisheries Sciences Hokkaido University* **69(2):**83–91 DOI 10.14943/bull.fish.69.2.83.

Hirakawa K, Imamura A. 1993. Seasonal abundance and life history of *Metridia pacifica* (Copepoda: Calanoida) in Toyama Bay, southern Japan Sea. *Bulletin of Plankton Society of Japan* **40(1)**:41–54 https://agriknowledge.affrc.go.jp/RN/2010511915.pdf

Homma T, Yamaguchi A. 2010. Vertical changes in abundance, biomass and community structure of copepods down to 3000 m in the southern Bering Sea. *Deep Sea Research Part I: Oceanographic Research Papers* **57(8)**:949–964 DOI 10.1016/j.dsr.2010.05.002.

Honda MC, Wakita M, Matsumoto K, Fujiki T, Siswanto E, Sasaoka K, Kawakami H, Mino Y, Sukigara C, Kitamura M, Sasai Y, Smith SL, Hashioka T, Yoshikawa C, Kimoto K, Watanabe S, Kobari T, Nagata T, Hamasaki K, Kaneko R, Uchimiya M, Fukuda H, Abe O, Saino T. 2017. Comparison of carbon cycle between the western Pacific subarctic and subtropical time-series stations: highlights of the K2S1 project. *Journal of Oceanography* **73(5)**:647–667 DOI /10.1007/s10872-017-0423-3.

Ikeda T, Hirakawa K. 1996. Early development and estimated life cycle of the mesopelagic copepod *Pareuchaeta elongata* in the southern Japan Sea. *Marine Biology* **126(2)**:261–270 DOI 10.1007/BF00347451.

Ikeda T, Shiga N, Yamaguchi A. 2008. Structure, biomass distribution and trophodynamics of the pelagic ecosystem in the Oyashio region, western subarctic Pacific. *Journal of Oceanography* **64(3)**:339–354 DOI 10.1007/s10872-008-0027-z.

Irisson J-O, Ayata S-D, Lindsay DJ, Karp-Boss L, Stemmann L. 2022. Machine learning for the study of plankton and marine snow from images. *Annual Review of Marine Science* **14:**277–301 DOI 10.1146/annurev-marine-041921-013023.

Kitamura M, Kobari T, Honda MC, Matsumoto K, Sasaoka K, Nakamura R, Tanabe K. 2016. Seasonal changes in the mesozooplankton biomass and community structure in subarctic and subtropical time-series stations in the western North Pacific. *Journal of Oceanography* **72(5)**:387–402 DOI 10.1007/s10872-015-0347-8.

Kobari T, Ikeda T. 2000. Life cycle of *Neocalanus* species in the Oyashio region. *Bulletin of the Plankton Society of Japan* **47(2)**:129–135. https://agriknowledge.affrc.go.jp/RN/2010620369.pdf

Kobari T, Steinberg DK, Ueda A, Tsuda A, Silver MW, Kitamura M. 2008. Impacts of ontogenetically migrating copepods on downward carbon flux in the western subarctic Pacific Ocean. *Deep-Sea Research Part II: Topical Studies in Oceanography* **55(14–15)**:1648–1660 DOI 10.1016/j.dsr2.2008.04.016.

Koguchi Y, Tokuhiro K, Ashjian CJ, Campbell RG, Yamaguchi A. 2023. Body length, dry and ash-free dry weights, and developmental changes at each copepodid stage in five sympatric mesopelagic aetideid copepods in the western Arctic Ocean. *Crustaceana* **96(2)**:113–129 DOI 10.1163/15685403-bja10272.

Krause EP, Lewis AG. 1979. Ontogenetic migration and the distribution of *Eucalanus bungii* (Copepoda; Calanoida) in British Columbia inlets. *Canadian Journal of Zoology* **57(11)**:2211–2222 DOI 10.1139/z79-288.

Mauchline J. 1998. The biology of calanoid copepods. *Advances in Marine Biology* **33**:1–710 DOI 10.1086/393440.

Miller CB, Frost BW, Batchelder HP, Clemons MJ, Conway RE. 1984. Life histories of large, grazing copepods in a subarctic ocean gyre: *Neocalanus plumchrus*, *Neocalanus cristatus*, and *Eucalanus bungii* in the Northeast Pacific. *Progress in Oceanography* **13(2)**:201–243 DOI 10.1016/0079-6611(84)90009-0.

Naito A, Abe Y, Matsuno K, Nishizawa B, Kanna N, Sugiyama S, Yamaguchi A. 2019. Surface zooplankton size and taxonomic composition in Bowdoin Fjord, north-western Greenland: A comparison of ZooScan, OPC, and microscopic analyses. *Polar Science* **19**:120–129 DOI 10.1016/j.polar.2019.01.001.

Nakamura Y, Zhang H, Yamaguchi A. 2023. Vertical distribution, community and population structures of the planktonic Chaetognatha in the western subarctic Pacific: Insights on the *Eukrohnia* species group. *Oceans*, **4(3)**:253–268 DOI 10.3390/oceans4030018.

Padmavati G, Ikeda T, Yamaguchi A. 2004. Life cycle, population structure and vertical distribution of *Metridia* spp. (Copepoda: Calanoida) in the Oyashio region (NW Pacific Ocean). *Marine Ecology Progress Series* **270**:181–198 DOI 10.3354/meps270181.

Sato K, Yamaguchi A, Ueno H, Ikeda T. 2011. Vertical segregation within four grazing copepods in the Oyashio region during early spring. *Journal of Plankton Research* **33(8)**:1230–1238 DOI 10.1093/plankt/fbr018.

Shoden S, Ikeda T, Yamaguchi A. 2005. Vertical distribution, population structure and life cycle of *Eucalanus bungii* (Copepoda: Calanoida) in the Oyashio region, with notes on its regional variations. *Marine Biology* **146(3)**:497–511 DOI 10.1007/s00227-004-1450-3.

Steinberg DK, Cope JS, Wilson SE, Kobari T. 2008a. A comparison of mesopelagic mesozooplankton community structure in the subtropical and subarctic North Pacific Ocean. *Deep Sea Research Part II: Topical Studies in Oceanography* **55(14–15)**:1615–1635 10.1016/j.dsr2.2008.04.025.

Steinberg DK, Van Mooy BAS, Buesseler KO, Boyd PW, Kobari T, Karl DM. 2008b. Bacterial vs. zooplankton control of sinking particle flux in the ocean's twilight zone. *Limnology and Oceanography* **53(4)**:1327–1338 DOI 10.4319/lo.2008.53.4.1327.

Takahashi K, Kuwata A, Sugisaki H, Uchikawa K, Saito H. 2009. Downward carbon transport by diel vertical migration of the copepods *Metridia pacifica* and *Metridia okhotensis* in the Oyashio region of the western subarctic Pacific Ocean. *Deep Sea Research Part I: Oceanographic Research Papers* **56(10)**:1777–1791 DOI 10.1016/j.dsr.2009.05.006.

Taniguchi R, Amei K, Tokuhiro K, Yamada Y, Kitamura M, Yamaguchi A. 2023. Diel, seasonal and vertical changes in the pelagic amphipod communities in the subarctic Pacific: Insights from imaging analysis. *Journal of Plankton Research* **45(3)**:554–570 DOI 10.1093/plankt/fbad017.

Teraoka T, Amei K, Fukai Y, Matsuno K, Onishi H, Ooki A, Takatsu T, Yamaguchi A. 2022. Seasonal changes in taxonomic, size composition, and Normalized Biomass Size Spectra (NBSS) of mesozooplankton communities in Funka Bay, southwestern Hokkaido: Insights from ZooScan analysis. *Plankton and Benthos Research* **17(4)**:369–382 DOI 10.3800/pbr.17.369.

Tsuda A, Saito H, Kasai H. 2004. Life histories of *Eucalanus bungii* and *Neocalanus cristatus* (Copepoda: Calanoida) in the western subarctic Pacific Ocean. *Fisheries Oceanography* **13(Suppl.1)**:10–20 DOI 10.1111/j.1365-2419.2004.00315.x.

Yamaguchi A, Ikeda T. 2000a. Vertical distribution, life cycle, and developmental characteristics of the mesopelagic calanoid copepod *Gaidius variabilis* (Aetideidae) in the Oyashio region, western North Pacific Ocean. *Marine Biology* **137(1)**:99–109 DOI 10.1007/s002270000316.

Yamaguchi A, Ikeda T. 2000b. Vertical distribution, life cycle and body allometry of two oceanic calanoid copepods (*Pleuromamma scutullata* and *Heterorhabdus tanneri*) in the Oyashio region, western North Pacific Ocean. *Journal of Plankton Research* **22(1)**:29–46 DOI 10.1093/plankt/22.1.29.

Yamaguchi A, Ikeda T. 2002. Reproductive and developmental characteristics of three mesopelagic *Paraeuchaeta* species (Copepoda: Calanoida) in the Oyashio region, western subarctic Pacific Ocean. *Bulletin of Fisheries Sciences Hokkaido University* **53(1)**:11–21. http://hdl.handle.net/2115/21959

Yamaguchi A, Watanabe Y, Ishida H, Harimoto T, Furusawa K, Suzuki S, Ishizaka J, Ikeda T, Takahashi M. 2002. Community and trophic structures of pelagic copepods down to greater depths in the western subarctic Pacific (WEST-COSMIC). *Deep Sea Research Part I: Oceanographic Research Papers* **49(6)**, 1007–1025 DOI 10.1016/S0967-0637(02)00008-0.

Yamaguchi A, Ikeda T, Watanabe Y, Ishizaka J. 2004. Vertical distribution patterns of pelagic copepods as viewed from the predation pressure hypothesis. *Zoological Studies* **43(2)**:475–485. https://zoolstud.sinica.edu.tw/Journals/43.2/475.pdf

Yamaguchi A, Tachibana S, Hirakawa K, Ikeda T. 2005. Descriptions of the copepodid stages of the mesopelagic copepod, *Gaetanus variabilis* (Brodsky, 1950) (Calanoida, Aetideidae) from the Japan Sea. *Crustaceana* **78(7)**:819–837 DOI 10.1163/156854005774445447.

Yamaguchi A, Onishi Y, Omata A, Kawai M, Kaneda M, Ikeda T. 2010a. Population structure, egg production and gut content pigment of large grazing copepods during the spring phytoplankton bloom in the Oyashio region. *Deep Sea Research Part II: Topical Studies in Oceanography* **57(17–18)**:1679–1690 DOI 10.1016/j.dsr2.2010.03.012.

Yamaguchi A, Onishi Y, Kawai M, Omata A, Kaneda M, Ikeda T. 2010b. Diel and ontogenetic variations in vertical distributions of large grazing copepods during the spring phytoplankton bloom in the Oyashio region. *Deep Sea Research Part II: Topical Studies in Oceanography* **57(17–18)**:1691–1702 DOI 10.1016/j.dsr2.2010.03.013.

Yamaguchi A, Ashjian CJ, Campbell RG, Abe Y. 2019. Ontogenetic vertical migration of the mesopelagic carnivorous copepod *Paraeuchaeta* spp. is related to their increase in body mass. *Journal of Plankton Research* **41(5)**:791–797 DOI 10.1093/plankt/fbz051.

Yamaguchi A, Ashjian CJ, Campbell RG, Abe Y. 2020. Vertical distribution, population structure and developmental characteristics of the less studied but globally distributed mesopelagic copepod *Scaphocalanus magnus* in the western Arctic Ocean. *Journal of Plankton Research* **42(3)**:368–377 DOI 10.1093/plankt/fbaa021.

Yokoi N, Abe Y, Kitamura M, Honda MC, Yamaguchi A. 2018. Comparisons between POC and zooplankton swimmer flux from sediment traps in the subarctic and subtropical North Pacific. *Deep Sea Research Part I: Oceanographic Research Papers* **133**:19–26 DOI 10.1016/j.dsr.2018.01.003.

Table 1(on next page)

Sampling data at St. K2 in the western subarctic Pacific during October 2010 to July 2021.

All the samples were collected from eight discrete depths between 0 and 1000 m (0–50, 50–100, 100–150, 150–200, 200–300, 300–500, 500–750, 750–1000 m) by oblique tow of IONESS.

1

Table 1. Sampling data at St. K2 in the western subarctic Pacific during October 2010 to July 2021. All the samples were collected from eight discrete depths between 0 and 1000 m (0–50, 50–100, 100–150, 150–200, 200–300, 300–500, 500–750, 750–1000 m) by oblique tow of IONESS.

Sampling date	Local time	D/N
29 Oct. 2010	12:09–13:52	D
29 Oct. 2010	22:09–23:38	N
26 Feb. 2011	12:35–14:41	D
26 Feb. 2011	22:01–23:44	N
22 Apr. 2011	21:59–23:56	N
22 Apr. 2011	12:45–14:37	D
3 July 2011	12:05–13:55	D
3/4 July 2011	22:51–0:55	N

2

Figure 1

Figure 1. Location of the sampling station (K2) in the western subarctic Pacific gyre.

Arrows represent approximate positions and directions of the currents (cf. Yasuda, 2003). EKC: East Kamchatka Current, OY: Oyashio , KE: Kuroshio Extension, TC: Tsushima Warm Current, SAF: Subarctic Front, SAB: Subarctic Boundary, KBF: Kuroshio Bifurcation Front, OSMW: Okhotsk Sea Mode Water, DSW: Dense Shelf Water, OSMW: Okhotsk Sea Mode Water.

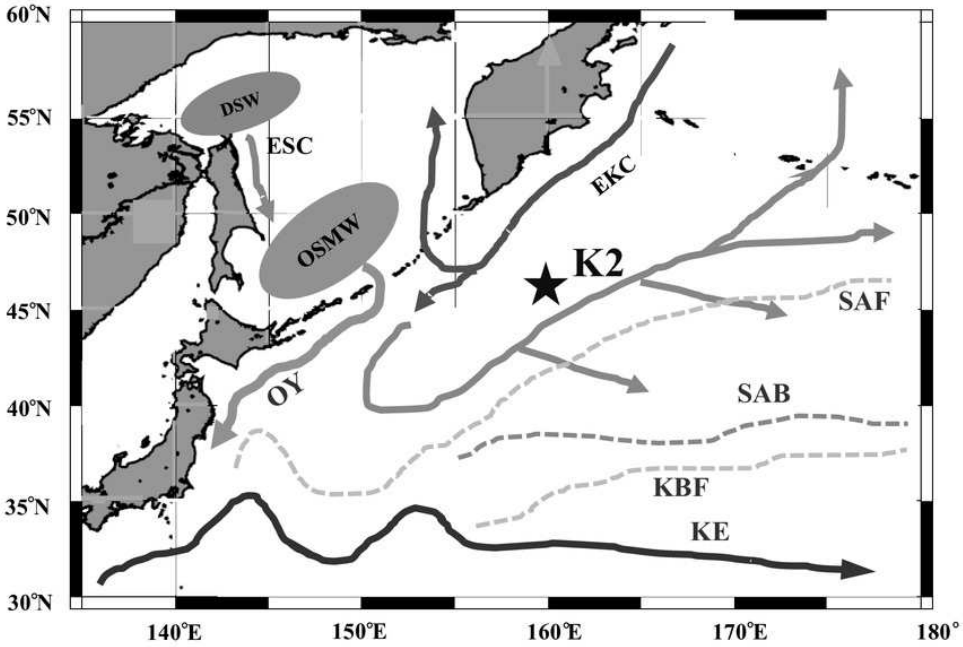

Figure 1. Location of the sampling station (K2) in the western subarctic Pacific gyre. Arrows represent approximate positions and directions of the currents (cf. Yasuda, 2003). EKC: East Kamchatka Current, OY: Oyashio, KE: Kuroshio Extension, TC: Tsushima Warm Current, SAF: Subarctic Front, SAB: Subarctic Boundary, KBF: Kuroshio Bifurcation Front, OSMW: Okhotsk Sea Mode Water, DSW: Dense Shelf Water, OSMW: Okhotsk Sea Mode Water.

Figure 2

Figure 2. ZooScan images of two treated general / species in this study: Metridia spp. (a) and Eucalanus bungii (b).

All copepodite stages were captured for M. pacifica and E. bungii . Note that scale bars are varied between (a) and (b). F: female, M: male.

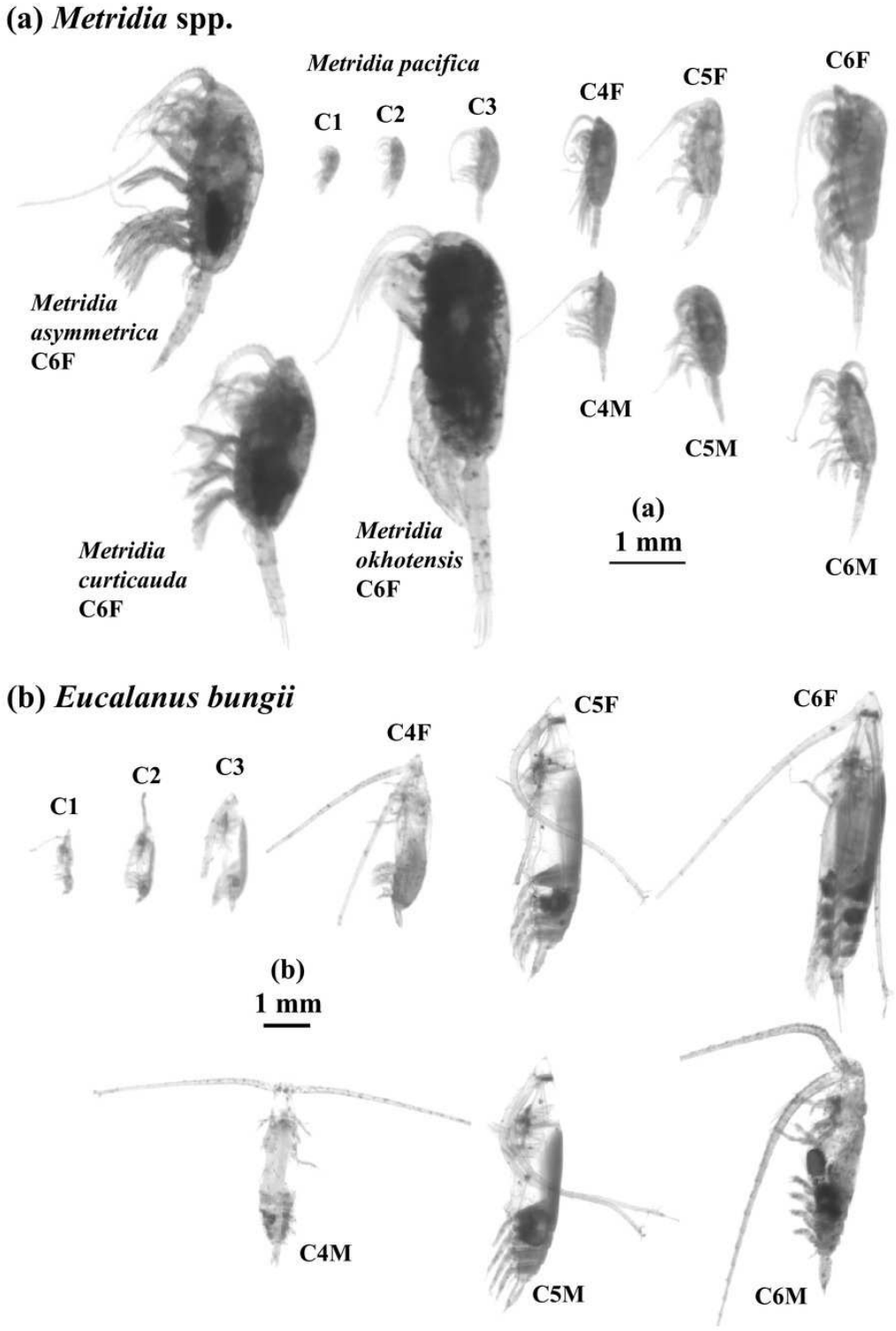

Figure 2. ZooScan images of two treated general/species in this study: *Metridia* spp. (a) and *Eucalanus bungii* (b). All copepodite stages were captured for *M. pacifica* and *E. bungii*. Note that scale bars are varied between (a) and (b). F: female, M: male.

Figure 3

Figure 3. Vertical changes in temperature (T), salinity (S), dissolved oxygen (O_2) and fluorescence (F) at St. K2 in the western subarctic Pacific from October 2010 to June 2011.

Circled numbers in the right column indicate the depth strata of the zooplankton sampling.

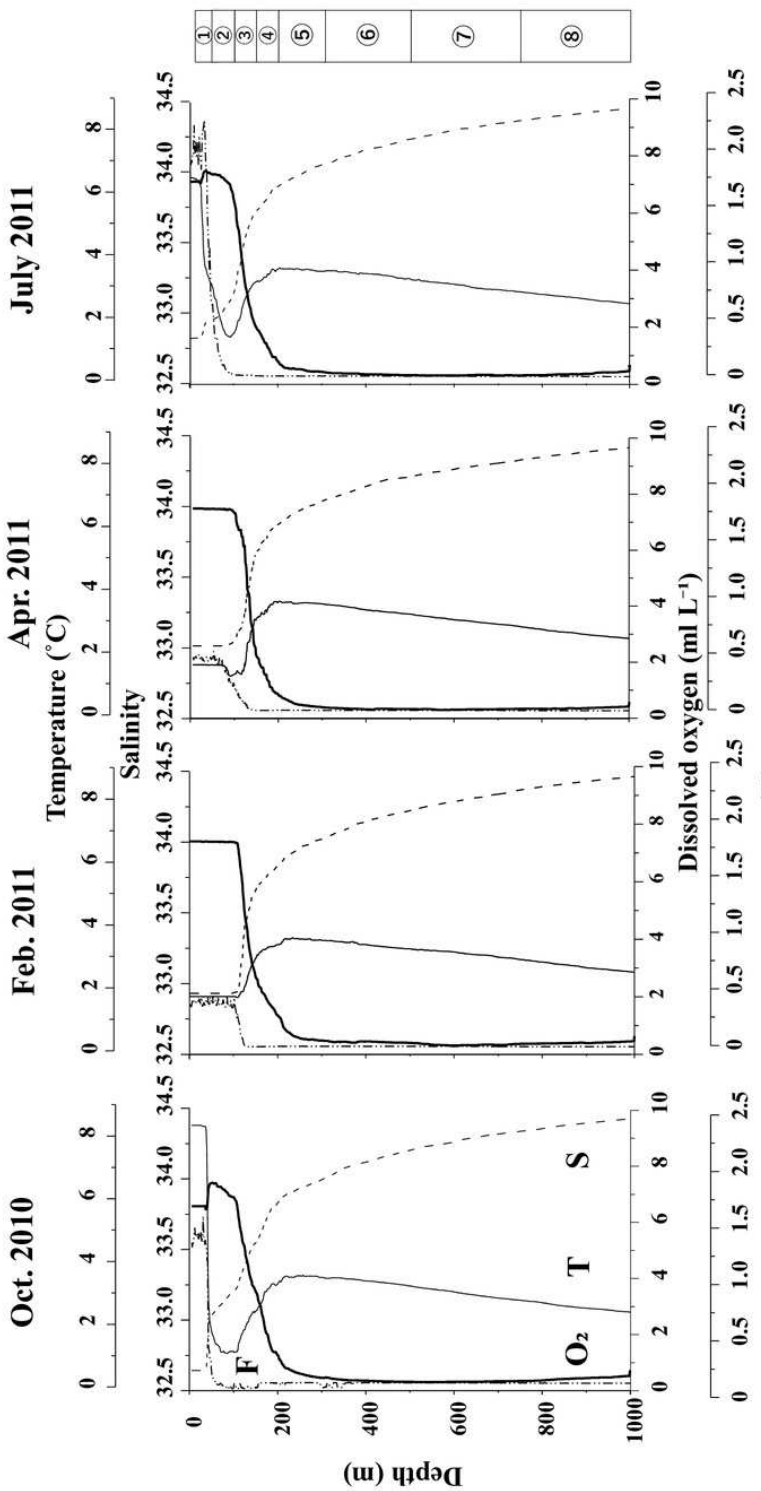

Figure 3. Vertical changes in temperature (T), salinity (S), dissolved oxygen (O_2) and fluorescence (F) at St. K2 in the western subarctic Pacific from October 2010 to June 2011. Circled numbers in the right column indicate the depth strata of the zooplankton sampling.

Figure 4

Figure 4. Metridia spp.: Abundance (ind. m -2), biovolume (mm 3 m -2), and their vertical distribution composition (%) at eight discrete depths along with the equivalent spherical diameter (ESD) at station K2 in the western subarctic Pacific

For the bottom panel, the mean (symbol) and standard deviation (bar) of the ESD of each stage Metridia pacipica and adult female of other Metridia species are shown for reference. M. pacifica (Mp), M. okhotensis (Mo), M. asymmetrida (Ma), and M. curticauda (Mc). F: female, M: male.

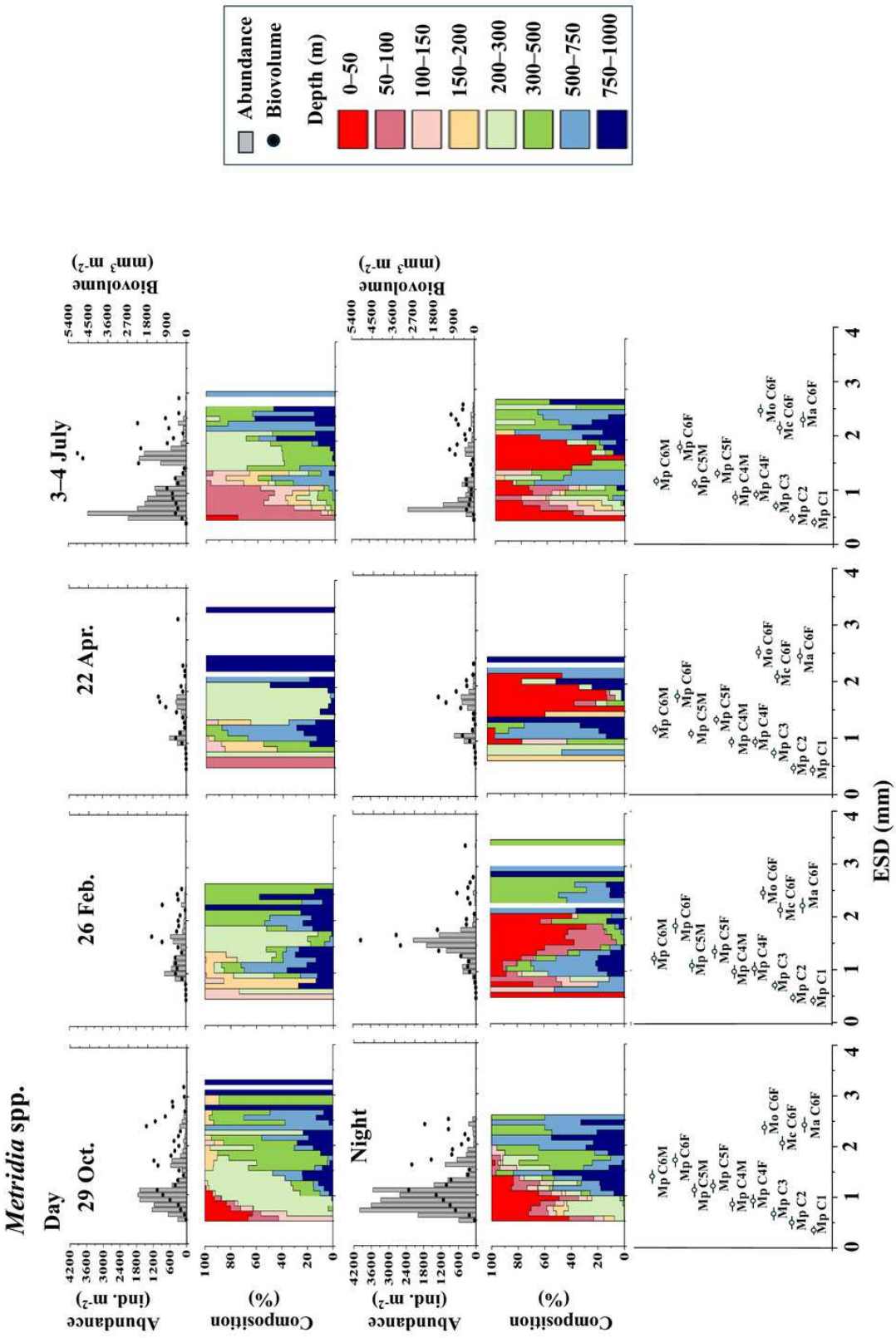

Figure 4. *Metridia* spp.: Abundance (ind. m^{-2}), biovolume (mm^3 m^{-2}), and their vertical distribution composition (%) at eight discrete depths along with the equivalent spherical diameter (ESD) at station K2 in the western subarctic Pacific during day (upper) and night (lower) of the four sampling dates: 29 October 2010, 26 February, 22 April, and 3-4 July 2011. For the bottom panel, the mean (symbol) and standard deviation (bar) of the ESD of each stage *Metridia pacipica and adult female of other Metridia* species are shown for reference. *M. pacifica* (Mp), *M. okhotensis* (Mo), *M. asymmetrida* (Ma), and *M. curticauda* (Mc). F: female, M: male.

Figure 5

Figure 5. Eucalanus bungii : Abundance (ind. m -2), biovolume (mm 3 m -2), and their vertical distribution composition (%) at eight discrete depths along with the equivalent spherical diameter (ESD) at station K2 in the western subarctic P

For the bottom panel, the mean (symbol) and standard deviation (bar) of the ESD of each copepodite stage of E. bungii are shown. F: female, M: male.

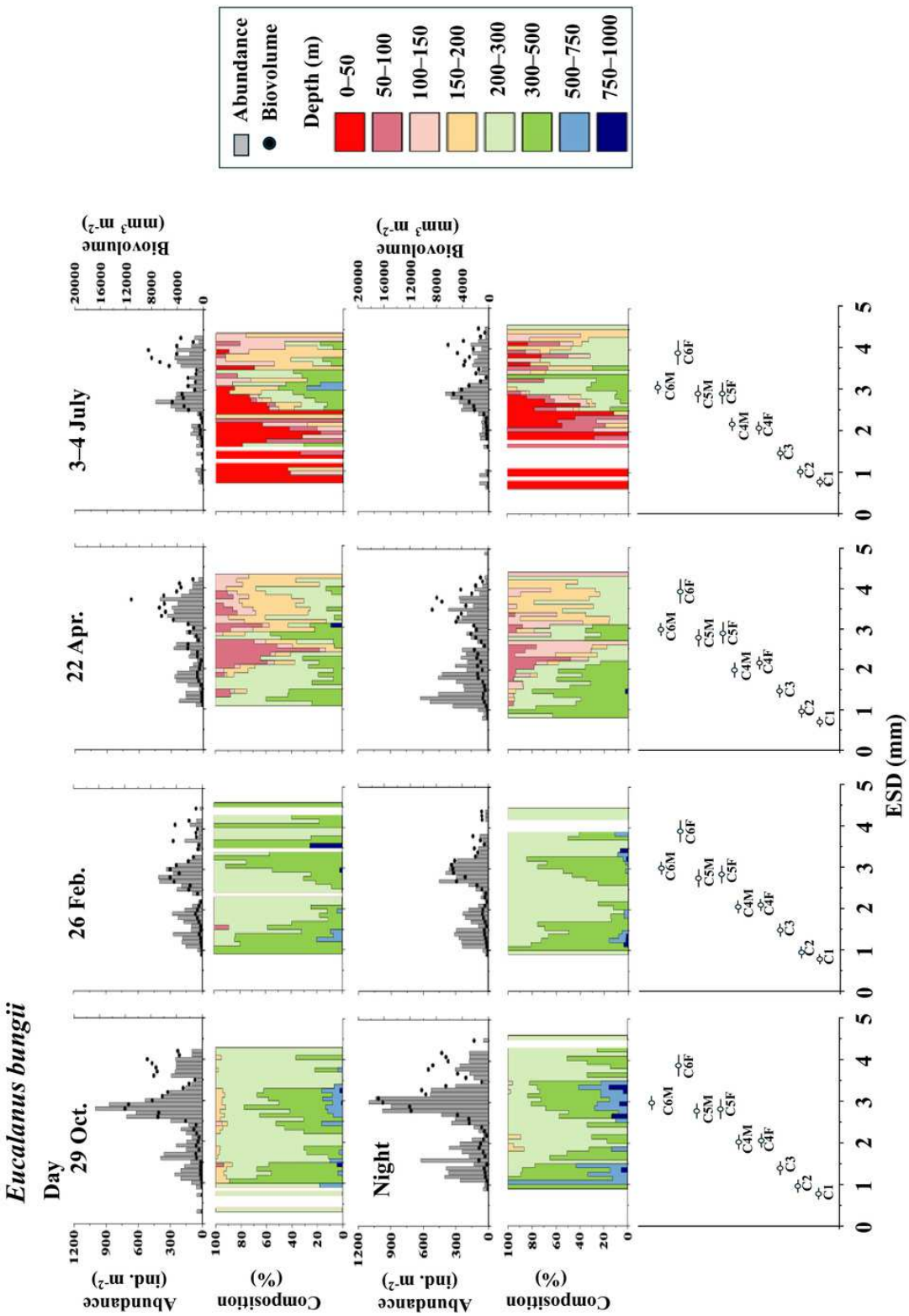

Figure 5. *Eucalanus bungii*: Abundance (ind. m^{-2}), biovolume (mm^3 m^{-2}), and their vertical distribution composition (%) at eight discrete depths along with the equivalent spherical diameter (ESD) at station K2 in the western subarctic Pacific during day (upper) and night (lower) of the four sampling dates: 29 October 2010, 26 February, 22 April, and 3-4 July 2011. For the bottom panel, the mean (symbol) and standard deviation (bar) of the ESD of each copepodite stage of *E. bungii* are shown. F: female, M: male.

Figure 6

Figure 6. Molt increment in terms of the equivalent spherical diameter (ESD, mm) and biovolume (mm 3 ind -1) of Metridia pacifica (a) and Eucalanus bungii (b) at station K2 in the western subarctic Pacific.

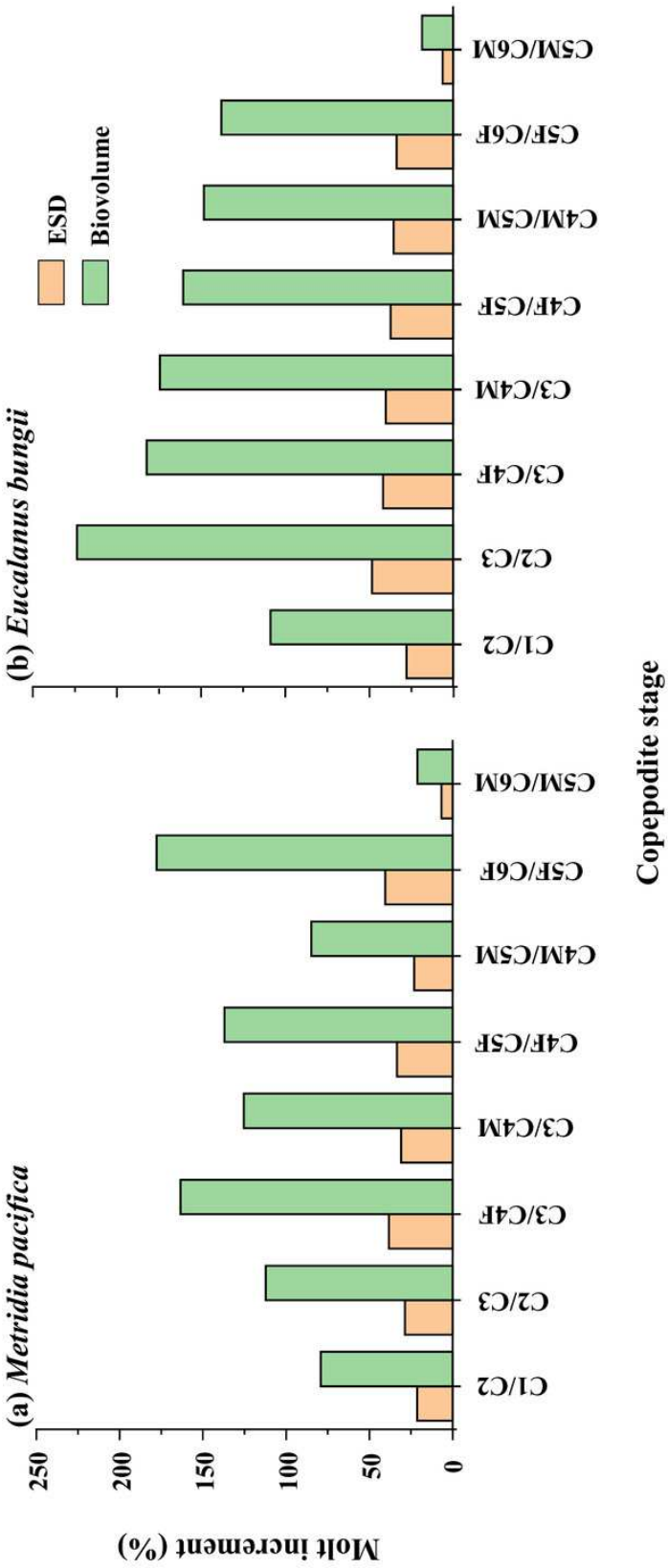

Figure 6. Molt increment in terms of the equivalent spherical diameter (ESD, mm) and biovolume (mm^3 ind^{-1}) of *Metridia pacifica* (a) and *Eucalanus bungii* (b) at station K2 in the western subarctic Pacific.

Figure 7

Figure 7. Proportion of growth at each stage molt in terms of the equivalent spherical diameter (ESD, mm) and biovolume (mm 3 ind. -1) of Metridia pacifica (a) and Eucalanus bungii (b) at station K2 in the western subarctic Pacif

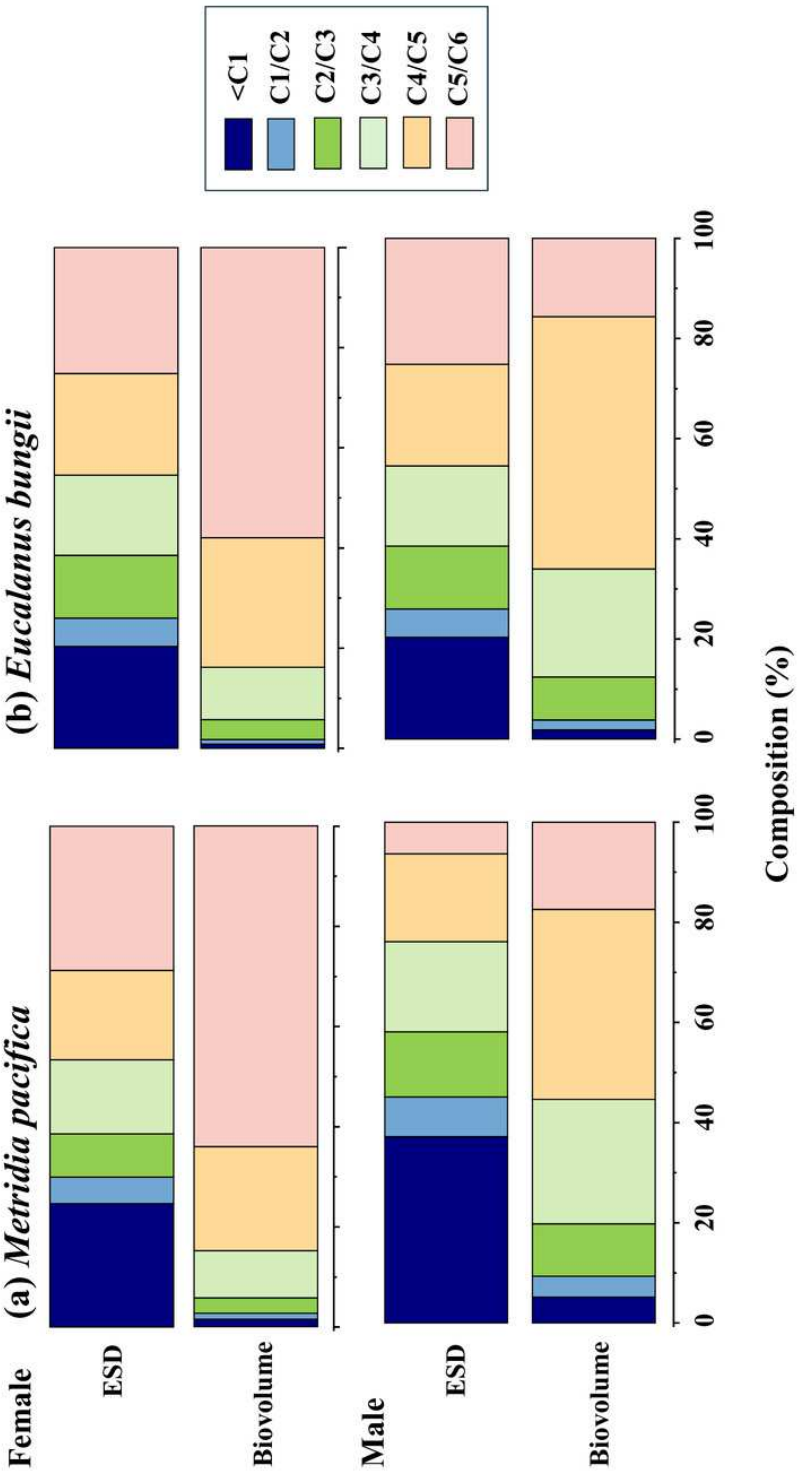

Figure 7. Proportion of growth at each stage molt in terms of the equivalent spherical diameter (ESD, mm) and biovolume (mm^3 $ind.^{-1}$) of *Metridia pacifica* (a) and *Eucalanus bungii* (b) at station K2 in the western subarctic Pacific.